

## SDSS J141624.08+134826.7: BLUE L DWARFS AND NON-EQUILIBRIUM CHEMISTRY

MICHAEL C. CUSHING<sup>1</sup>

Jet Propulsion Laboratory, California Institute of Technology, MS 264-723, 4800 Oak Grove Drive, Pasadena, CA 91109

D. SAUMON

Los Alamos National Laboratory, Applied Physics Division, MS F663, Los Alamos, NM 87545, dsaumon@lanl.gov

MARK S. MARLEY

NASA Ames Research Center, MS 254-3, Moffett Field, CA 94035, Mark.S.Marley@NASA.gov

*Draft version August 21, 2018*

### ABSTRACT

We present an analysis of the recently discovered blue L dwarf SDSS J141624.08+134826.7. We extend the spectral coverage of its published spectrum to  $\sim 4 \mu\text{m}$  by obtaining a low-resolution  $L$  band spectrum with SpeX on the NASA IRTF. The spectrum exhibits a tentative weak  $\text{CH}_4$  absorption feature at  $3.3 \mu\text{m}$  but is otherwise featureless. We derive the atmospheric parameters of SDSS J141624.08+134826.7 by comparing its  $0.7\text{--}4.0 \mu\text{m}$  spectrum to the atmospheric models of Marley and Saumon which include the effects of both condensate cloud formation and non-equilibrium chemistry due to vertical mixing and find the best fitting model has  $T_{\text{eff}}=1700 \text{ K}$ ,  $\log g=5.5 [\text{cm s}^{-2}]$ ,  $f_{\text{sed}}=4$ , and  $K_{\text{zz}}=10^4 \text{ cm}^2 \text{ s}^{-1}$ . The derived effective temperature is significantly cooler than previously estimated but we confirm the suggestion by Bowler et al. that the peculiar spectrum of SDSS J141624.08+134826.7 is primarily a result of thin condensate clouds. In addition, we find strong evidence of vertical mixing in the atmosphere of SDSS J141624.08+134826.7 based on the absence of the deep  $3.3 \mu\text{m}$   $\text{CH}_4$  absorption band predicted by models computed in chemical equilibrium. This result suggests that observations of blue L dwarfs are an appealing way to quantitatively estimate the vigor of mixing in the atmospheres of L dwarfs because of the dramatic impact such mixing has on the strength of the  $3.3 \mu\text{m}$   $\text{CH}_4$  band in the emergent spectra of L dwarfs with thin condensate clouds.

*Subject headings:* infrared: stars — stars: low-mass, brown dwarfs — subdwarfs — stars: individual (SDSS J141624.08+134826.7)

### 1. INTRODUCTION

Field L dwarfs (Kirkpatrick et al. 1999; Kirkpatrick 2005) comprise a mix of very low-mass stars and brown dwarfs. Although effective temperature ( $T_{\text{eff}}$ ) is the primary atmospheric parameter that controls their emergent spectra and thus their spectral type (e.g., Kirkpatrick 2008), secondary parameters such as surface gravity ( $g$ ) and metallicity  $[\text{Fe}/\text{H}]$ , as well as the condensate clouds properties and photospheric vertical mixing also play an important role. This is perhaps best illustrated by the fact that the  $J - K_s$  colors of L dwarfs can vary by up to 1 mag at a given spectral type (Leggett et al. 2002; Knapp et al. 2004; Chiu et al. 2006; Kirkpatrick 2008; Faherty et al. 2009; Schmidt et al. 2010b). Low metallicity explains the outliers with extreme blue  $J - K_s$  colors, but the relative importance of variations in metallicity, surface gravity, condensate cloud properties, and the vigor of vertical mixing to the bulk of the variation remains unknown.

L dwarfs that exhibit bluer than average colors also appear to exhibit peculiar spectral features including

enhanced FeH, K I, and  $\text{H}_2\text{O}$  absorption (Cruz et al. 2003; Knapp et al. 2004; Chiu et al. 2006; Cruz et al. 2007; Folkes et al. 2007; Burgasser et al. 2008a). All of the secondary parameters described above, along with unresolved binary, have been invoked to explain these spectral features. Burgasser et al. (2008a) performed a detailed analysis of the red-optical and near-infrared spectra of the blue L dwarf 2MASS J11263991–5003550 (hereafter 2MASS J1126–50) and found that thin condensate clouds provided the overall best explanation of its spectral properties. However, since the properties of the cloud model used in their analysis are encapsulated in a free parameter, it is still unclear which, if any, of the secondary parameters is the underlying physical cause of thin condensate clouds. More recent work by Faherty et al. (2009) and Schmidt et al. (2010b) have shown the blue L dwarfs have kinematics consistent with old age, suggesting that surface gravity and/or low-metallicity may account for their blue colors.

A common proper motion system consisting of a blue L dwarf SDSS J141624.08+134826.7 (hereafter SDSS J1416+13A, Schmidt et al. 2010a; Bowler et al. 2010; Burningham et al. 2010a) and a blue T dwarf ULAS J141623.94+134836.3 (hereafter SDSS J1416+13B, Scholz 2010; Burningham et al. 2010b) separated by  $9''$  was recently discovered that may shed some light on the underlying atmospheric

michael.cushing@gmail.com

<sup>1</sup> Visiting Astronomer at the Infrared Telescope Facility, which is operated by the University of Hawai'i under cooperative Agreement no. NCC 5-538 with the National Aeronautics and Space Administration, Office of Space Science, Planetary Astronomy Program.

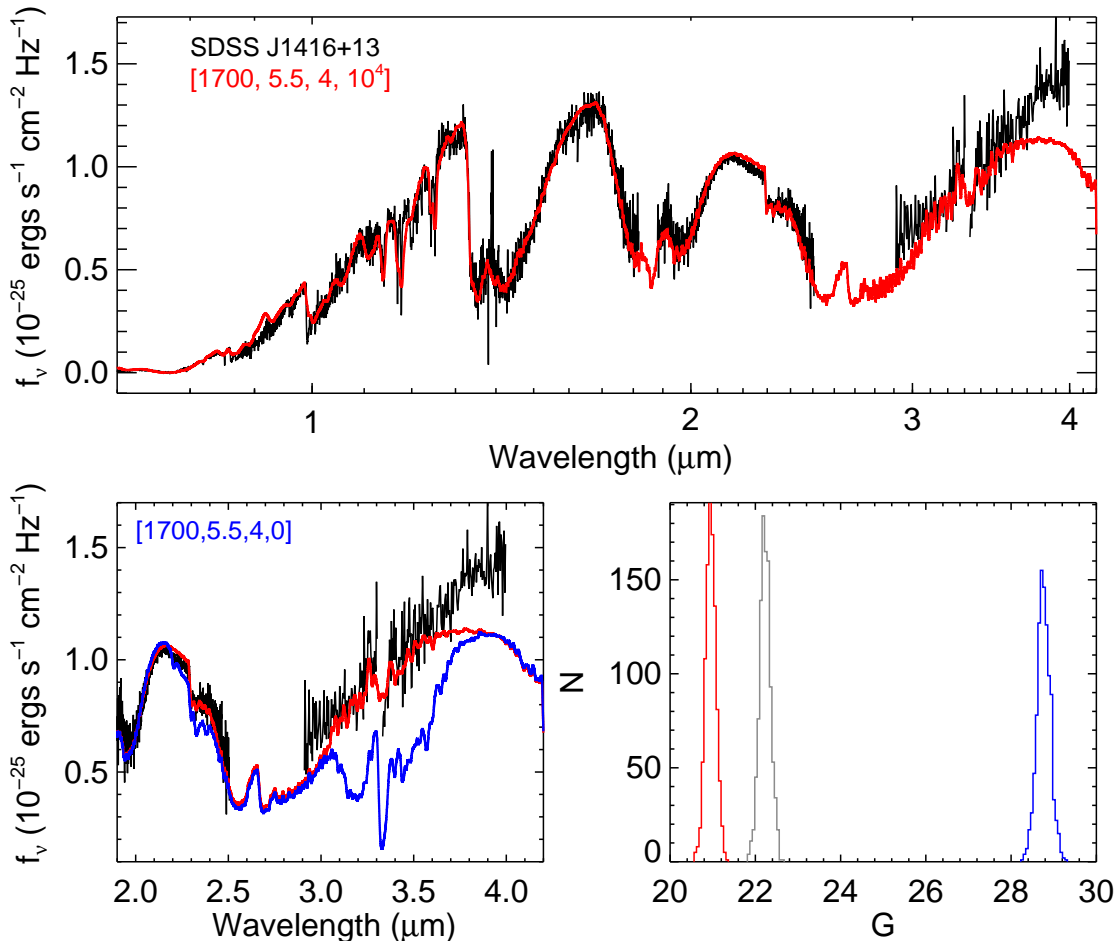


FIG. 1.— *Top*: 0.8–4.0  $\mu\text{m}$  spectrum of SDSS J1416+13A (black) overlotted with the best fitting model (red) with  $T_{\text{eff}}=1700$  K,  $\log g=5.5$  [ $\text{cm s}^{-1}$ ],  $f_{\text{sed}}=4$ ,  $K_{\text{zz}}=10^4$   $\text{cm}^2 \text{s}^{-1}$  [1700, 5.5, 4,  $10^4$ ]. *Lower left*: Same as top panel except the model with  $K_{\text{zz}}=0$   $\text{cm}^2 \text{s}^{-1}$  is shown in blue. Note that for display purposes, the models are shown at a lower resolution. *Lower right*: Distribution of  $G$  values for the best fitting model [1700, 5.5, 4,  $10^4$ ] in red, the second best-fitting model [1800, 5.5, 4, 0] in grey, and the model with  $K_{\text{zz}}=0$   $\text{cm}^2 \text{s}^{-1}$  (blue) shown in the lower left panel.

physics of the blue L dwarfs. Based on its red optical spectrum, Bowler et al. (2010) and Schmidt et al. (2010a) classify SDSS J1416+13A as a dwarf (L6 and L5 respectively), while Burningham et al. (2010b) classify it as a dwarf/subdwarf (d/sdL7) and Kirkpatrick et al. (2010) classify it as a subdwarf (sdL7). The subdwarf classifications suggest metallicity may play a role in explaining the properties of the blue L dwarfs but the disparate spectral types only underscores the difficulty of separating the effects of gravity, metallicity, and the condensate clouds properties. Using model atmospheres Burgasser et al. (2010) found that the near-infrared spectrum of SDSS J1416+13B was consistent with a subsolar metallicity of  $[\text{Fe}/\text{H}] \leq -0.3$  and high surface gravity of  $\log g = 5.2 \pm 0.4$  [ $\text{cm s}^{-2}$ ]. Since we can reasonably assume that SDSS J1416+13A and SDSS J1416+13B are coeval and have the same composition, this analysis provides the first concrete evidence that metallicity and/or surface gravity are the secondary parameters controlling the spectra of the blue L dwarfs.

In this paper, we extended the spectral coverage of the spectrum of SDSS J1416+13A to 4  $\mu\text{m}$  and derive its atmospheric parameters by comparing its 0.7–4.0  $\mu\text{m}$  spec-

trum to the atmospheric models of Marley and Saumon (Marley et al. 2002; Saumon & Marley 2008). We confirm the suggestion of Bowler et al. (2010) that the spectral peculiarities of SDSS J1416+13A are due to a thin condensate cloud and find strong evidence for vertical mixing in the atmosphere of SDSS J1416+13A.

## 2. OBSERVATIONS

A 1.9–4.0  $\mu\text{m}$  spectrum of SDSS J1416+13A was obtained on 2010 Jan 29 (UT) using SpeX (Rayner et al. 2003) on the 3 m NASA IRTF. We used the Long-Cross-Dispersed mode (LXD) with the 0'8 slit to obtain a spectrum at a resolving power  $R \equiv \lambda/\Delta\lambda \approx 940$ . A series of 15 sec exposures were obtained at two positions along the 15'' slit. We observed the A0 V star HD 121996 for telluric correction and flux calibration purposes. All observations were conducted at the parallactic angle even though slit losses and spectral slope variations due to differential atmospheric refraction are minimal at these wavelengths. Finally exposures of internal flat field and Ar arc lamps were obtained for flat fielding and wavelength calibration.

The data were reduced using Spextool, the IDL-based data reduction package for SpeX (Cushing et al. 2004) using standard procedures. The raw spectrum of SDSS

1416+13 was corrected for telluric correction and flux calibrated using the observed A0 V star and the technique described in Vacca et al. (2003). Regions of low signal-to-noise (S/N) at wavelengths with strong telluric absorption from 2.5 to 2.9  $\mu\text{m}$  and centered at 3.3  $\mu\text{m}$  were removed and the spectrum was rebinned to 1 pixel per resolution element resulting in a final S/N of  $\sim 15$ .

To construct a nearly complete 0.5–4.0  $\mu\text{m}$  spectrum of SDSS J1416+13A we combined our  $L$ -band spectrum with previously published red-optical and near-infrared spectra. The LXD spectrum was scaled to match the  $K$ -band flux level of the Schmidt et al. (2010a) 0.8–2.5  $\mu\text{m}$  SpeX spectrum ( $R=2000$ ,  $S/N=50$ –150) and the two spectra were averaged together. The red-optical SDSS spectrum was scaled to match the flux level of the merged spectrum and then averaged with the merged spectrum. The resulting 0.5–4.0  $\mu\text{m}$  spectrum was absolutely flux calibrated using published 2MASS photometry and the technique described in Rayner et al. (2009).

The spectrum, which is shown in the top panel of Figure 1, is consistent with the  $L$ -band spectra of other mid-type L dwarfs (Noll et al. 2000; Cushing et al. 2005; Stephens et al. 2009) in that it is relatively featureless at this resolution and S/N. There is a hint of absorption at 3.3  $\mu\text{m}$  due to the Q branch of the  $\nu_3$  band of  $\text{CH}_4$  but the telluric  $\text{CH}_4$  absorption makes this identification tentative.

We also computed the bolometric flux of SDSS J1416+13A using the flux calibrated spectrum. We first extended the spectrum blueward by extrapolating from the end of the SDSS spectrum at  $\sim 4000$   $\text{\AA}$  to zero flux at zero wavelength. Gaps in the spectrum were linearly interpolated over and we used the *Spitzer* Infrared Camera (IRAC) [4.5] photometry (Burningham et al. 2010a) and a Rayleigh-Jeans tail to account for the flux emitted at  $\lambda > 4$   $\mu\text{m}$ . Integrating over the spectrum yields  $f_{\text{bol}}=2.13\pm 0.04$   $\text{W m}^{-2}$  ( $m_{\text{bol}}=15.19\pm 0.02$ )<sup>2</sup> where the error is generated via a Monte Carlo simulation that includes the errors in the individual spectral points, the error in the IRAC magnitude, and the overall absolute flux calibration error of the spectrum. If instead, we use the best fitting model identified in the next section to account for the flux emitted at  $\lambda > 4.5$   $\mu\text{m}$  we find  $f_{\text{bol}}=2.11\pm 0.04$   $\text{W m}^{-2}$  which indicates that the assumed form of the flux distribution longward of 4.5  $\mu\text{m}$  is not a significant source of systematic error. This bolometric flux value can be used to compute the bolometric luminosity of SDSS J1416+13A when a precise parallax becomes available.

### 3. ANALYSIS: ATMOSPHERIC PARAMETERS

We compared the spectrum of SDSS J1416+13A to the model spectra of Marley et al. (2002) and Saumon & Marley (2008) in order to estimate its atmospheric parameters (see Cushing et al. (2008) and Stephens et al. (2009) for a more detailed description of the models). We used a grid of solar metallicity<sup>3</sup> models

<sup>2</sup>  $m_{\text{bol}} = -2.5 \times \log(f_{\text{bol}}) - 18.988$  assuming  $L_{\odot} = 3.86 \times 10^{26}$  W and  $M_{\text{bol}\odot} = +4.74$ .

<sup>3</sup> Burgasser et al. (2010) found that SDSS J1416+13B was slightly metal poor at  $[\text{Fe}/\text{H}]=-0.3$  and the dwarf/subdwarf and subdwarf spectral types of Burningham et al. (2010b) and Kirk-

patrick et al. (submitted) suggest SDSS J1416+13A has a subsolar metallicity. However nonsolar metallicity cloudy models are not currently available so we proceed with our analysis using only solar metallicity models.

with  $T_{\text{eff}}=1000$  to 2400 K in steps of 100 K,  $\log g=4.0, 4.5, 5.0, 5.5$  [ $\text{cm s}^{-2}$ ],  $f_{\text{sed}}=1, 2, 3, 4, \infty$  (no cloud), and  $K_{\text{zz}}=0, 10^4$   $\text{cm}^2 \text{s}^{-1}$ . The sedimentation efficiency  $f_{\text{sed}}$  (Ackerman & Marley 2001) parameterizes the efficiency of condensate sedimentation relative to turbulent mixing. Clouds with larger values of  $f_{\text{sed}}$  have larger modal particle sizes and thus are thinner. The eddy diffusion coefficient  $K_{\text{zz}}$  parameterizes the vigor of mixing in the radiative layers of the atmosphere and ranges from  $10^2$  to  $10^5$   $\text{cm}^2 \text{s}^{-1}$  in the stratospheres of giant planets (Saumon et al. 2006). The model spectra were smoothed to the spectral resolution of the data and interpolated onto the wavelength scale of the data.

We identified the best fitting model spectra in the grid using the goodness-of-fit statistic  $G_k$  described in Cushing et al. (2008, see also Bowler et al. (2009); Burgasser et al. (2008b)). We weighted each spectral point by its width in logarithmic wavelengths  $w_i = \delta \ln \lambda_i$ , but note that the results do not change if we give equal weights to all points ( $w_i = 1$ ). For each model  $k$ , we compute the scale factor  $C_k=(R/d)^2$ , where  $R$  and  $d$  are the radius and distance of the dwarf respectively, that minimizes  $G_k$ . The best fitting model is identified as having the global minimum  $G_k$  value. To estimate the uncertainty, we run a Monte Carlo simulation using both the uncertainties in the individual spectral points and the overall absolute flux calibration of the spectrum (see Cushing et al. 2008; Bowler et al. 2009; Burgasser et al. 2010).

The best fitting model has  $T_{\text{eff}}=1700$  K,  $\log g=5.5$  [ $\text{cm s}^{-2}$ ],  $f_{\text{sed}}=4$ , and  $K_{\text{zz}}=10^4$   $\text{cm}^2 \text{s}^{-1}$ , (hereafter [1700, 5.5, 4,  $10^4$ ]), and is shown in the top panel of Figure 1 overplotted on the spectrum of SDSS J1416+13A. The distribution of  $G$  values generated during the Monte Carlo simulation for the best-fitting model [1700, 5.5, 4,  $10^4$ ] and second best-fitting model with [1800, 5.5, 4, 0] are given in the lower right panel of Figure 1 and indicate that the best-fitting model is  $19 \sigma$  better than the second best-fitting model. Overall the model spectrum matches the data well in the 0.5–2.5  $\mu\text{m}$  wavelength range but it fails to match the shape of the  $L$ -band. In particular, the model turns over at 3.8  $\mu\text{m}$  while the data continue to rise to the limit of the observations at  $\sim 4$   $\mu\text{m}$ . This mismatch appears to be systemic (e.g., Cushing et al. 2008; Stephens et al. 2009) and is probably a result of the cloud model not producing enough small ( $\leq 1$   $\mu\text{m}$ ) particles, but a nonsolar metallicity cannot be ruled out.

The derived effective temperature of  $T_{\text{eff}}=1700$  K and surface gravity of  $\log g=5.5$  [ $\text{cm s}^{-2}$ ] are consistent with the values derived for other L dwarfs with similar spectral types (Cushing et al. 2008; Stephens et al. 2009; Testi 2009). The effective temperature of 1700 K is, however, substantially cooler than the 2200 K temperature derived by Bowler et al. (2010) using the AMES-dusty model atmospheres (Allard et al. 2001). The AMES-dusty models assume that the dust grains form in chemical equilibrium with the gas and do not gravitationally settle into clouds. As a result, AMES-dusty models with  $T_{\text{eff}}=1700$  K have extremely red near-infrared colors because of the

patrick et al. (submitted) suggest SDSS J1416+13A has a subsolar metallicity. However nonsolar metallicity cloudy models are not currently available so we proceed with our analysis using only solar metallicity models.

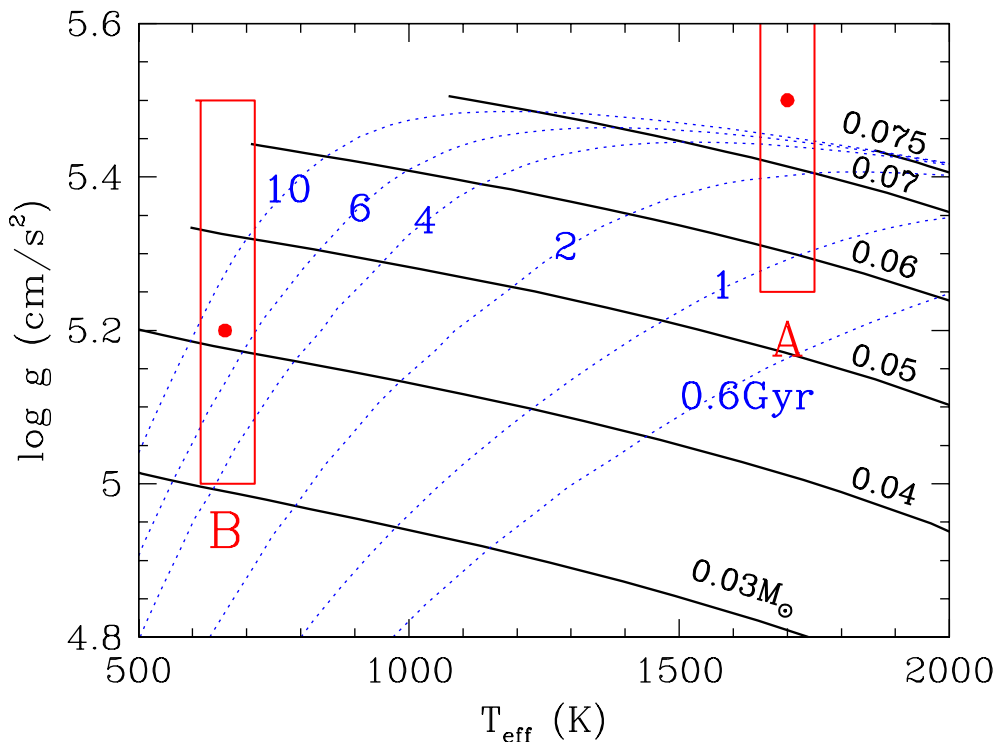


FIG. 2.— Age and masses of the two components of SDSS J1416+13A based on the  $(T_{\text{eff}}, g)$  derived from the analysis of their spectra and an evolution sequence using cloudless atmospheres and  $[M/H]=-0.3$  (Saumon & Marley 2008). The parameters of SDSS J1416+13A ( $T_{\text{eff}}=1700\pm 50$  K,  $\log g=5.5\pm 0.25$  [ $\text{cm s}^{-2}$ ]) are from this work, those of SDSS 1416+13B ( $T_{\text{eff}}=660^{+55}_{-45}$  K,  $\log g=5.2^{+0.3}_{-0.2}$  [ $\text{cm s}^{-2}$ ]) are from Burgasser et al. (2010). Isochrones are shown with blue dotted lines and are labeled with the age in Gyr. Black solid lines show the cooling for brown dwarfs with masses given in  $M_{\odot}$ . Isochrones with ages greater than 4 Gyr are consistent with the parameters derived from both objects.

large column of dust above the photosphere. An AMES-dusty model with a higher effective temperature (i.e., less dust) is therefore required to match the blue colors of SDSS J1416+13A.

The derived surface gravity of  $\log g=5.5$  [ $\text{cm s}^{-2}$ ] is not only at the edge of our model grid but is also somewhat high because at  $T_{\text{eff}}=1700$  K evolutionary models restrict the surface gravities of brown dwarfs to be  $< 5.42$  in the case of cloudless atmospheres and  $< 5.37$  in the case of cloudy ( $f_{\text{sed}}=2$ ) atmospheres (Saumon & Marley 2008). Nevertheless we continue to report results on the grid points because the model atmospheres were computed at these values. The high surface gravity supports the suggestion of Burgasser et al. (2010) that old age may be the underlying cause for the thin condensate clouds in the blue L dwarfs; however, the surface gravities of isolated field L dwarfs are notoriously difficult to measure precisely ( $\pm 0.25$  dex, Cushing et al. 2008) rendering any connection tentative at best.

The derived sedimentation efficiency of  $f_{\text{sed}}=4$  is high for an L dwarf as values of 1–3 are typical (Stephens et al. 2009). Indeed only one other L dwarf that has been fit with the Marley and Saumon models has  $f_{\text{sed}}=4$ : the blue L dwarf 2MASS J1126–50 (Burgasser et al. 2008a) discussed in §1. Unfortunately, the properties of the model condensate clouds are encapsulated in the free parameter  $f_{\text{sed}}$  which is set independently of the fundamental parameters  $g$  and  $[\text{Fe}/\text{H}]$  so no conclusion can be drawn regarding the underly-

ing physical mechanism for the thin clouds. However as noted in §1, the analysis of the T dwarf companion by Burgasser et al. (2010) suggests that the thin condensate clouds may be a result of the old age and/or metal poor atmosphere of SDSS J1416+13A. More theoretical work will be required before the cloud properties can be tied directly to the fundamental properties such as gravity and metallicity (Helling et al. 2001; Woitke & Helling 2003, 2004; Helling et al. 2004; Helling & Woitke 2006).

The derived eddy diffusion coefficient of  $K_{zz}=10^4$   $\text{cm}^2 \text{s}^{-1}$  is also at the edge of our model grid but does indicate the presence of vertical mixing in the atmosphere of SDSS J1416+13A. Although it is not surprising that such mixing is important in shaping the spectra of L dwarfs (Saumon et al. 2003, 2006, 2007; Leggett et al. 2007; Hubeny & Burrows 2007; Leggett et al. 2009; Stephens et al. 2009; Geballe et al. 2009; Leggett et al. 2010), the impact that the non-equilibrium carbon chemistry has on the  $3 \mu\text{m}$  spectral region is particularly dramatic in the case of SDSS J1416+13A. The lower left panel of Figure 1 shows the the  $K$  and  $L$ -band spectrum of SDSS J1416+13A, the best fitting model with  $[1700, 5.5, 4, 10^4]$ , and a model with the same  $T_{\text{eff}}$ ,  $\log g$ , and  $f_{\text{sed}}$ , but with  $K_{zz}=0$   $\text{cm}^2 \text{s}^{-1}$ . The model spectrum computed in chemical equilibrium exhibits a deep  $\text{CH}_4$  band at  $3.3 \mu\text{m}$  and a weak  $\text{CH}_4$  band at  $2.2 \mu\text{m}$ .

As a consistency check on the derived parameters, we estimated a spectroscopic parallax for SDSS J1416+13A

using the derived scale factor  $C_k$  (Bowler et al. 2009). We find that  $d/R=11.9\pm 0.07$  pc  $R_{\text{Jup}}^{-1}$  for the model with  $[1700, 5.5, 4, 10^4]$ , assuming the (equatorial) radius of Jupiter at 1 bar is 71492 km (Lindal et al. 1981). The cloudless evolutionary models of Saumon & Marley (2008) give  $R=0.81 R_{\text{Jup}}$  for  $T_{\text{eff}}=1700$  K and  $\log g=5.5$  [ $\text{cm s}^{-2}$ ] resulting in a distance estimate of  $9.7\pm 0.1$  pc<sup>4</sup>. The distance estimate is in good agreement with the parallactic ( $9.3\pm 3.0$  pc) and spectrophotometric ( $8.4\pm 1.9$  pc) distance estimates of Bowler et al. (2010) but lies just at the  $1\sigma$  limits of the Scholz (2010) parallactic distance estimate of  $7.9\pm 1.7$  pc and the Scholz (2010) spectrophotometric distance estimate of  $8.0\pm 1.6$  pc. The good agreement between our derived value and previous results implies that our derived atmospheric parameters are reasonable.

#### 4. DISCUSSION

As noted in §1, SDSS J1416+13A is a companion of the blue T dwarf SDSS J1416+13B (Scholz 2010; Burningham et al. 2010a) and thus it is reasonable to assume that the objects have a similar age and composition. Although we cannot test whether the metallicities of the two dwarfs are consistent, we can test that their ages inferred from evolutionary models are consistent. Figure 2 shows the cloudless evolutionary models with  $[M/H]=-0.3$  from Saumon & Marley (2008) along with the range of  $T_{\text{eff}}$  and  $\log g$  values derived for SDSS J1416+13A (this work) and SDSS J1416+13B (Burgasser et al. 2010). The uncertainty in the derived surface gravities translate into a large range of ages,  $\tau > 0.8$  Gyr in the case of SDSS J1416+13A and  $\tau > 3.2$  Gyr in the case of SDSS J1416+13B, but the derived ages are consistent with SDSS J1416+13A and SDSS J1416+13B being coeval. We note that using solar metallicity evolutionary models does not significantly change this conclusion.

Finally, although there is ample evidence that vertical mixing is important in the atmospheres of both L and T dwarfs, deriving precise values of  $K_{zz}$  has proven more difficult. Non-equilibrium chemistry affects both the carbon and nitrogen chemistry and thus the depths of the  $\text{CH}_4$  bands at 2.2 and 3.3  $\mu\text{m}$  (and to a lesser extent at 7.8  $\mu\text{m}$ ), the fundamental CO band at 4.7  $\mu\text{m}$ , and the fundamental  $\text{NH}_3$  band at 10.5  $\mu\text{m}$  (Saumon et al. 2003). However not all of these bands are sensitive to variations in the eddy diffusion coefficient  $K_{zz}$ . The  $\text{NH}_3$  abundance is quenched in convective layers of the atmosphere rendering the 10.5  $\mu\text{m}$  band insensitive to variations of  $K_{zz}$  in the radiative layers (Saumon et al. 2006). The fundamental CO band is sensitive to variations in  $K_{zz}$  but only four ground-based spectroscopic observations of T dwarfs (Noll et al. 1997; Oppenheimer et al. 1998; Geballe et al. 2009) at these wavelengths have been made due to the difficulty observing with such a high thermal background. In the absence of spectroscopy, *Spitzer* photometry of L and T dwarfs at 4.5  $\mu\text{m}$  with the Infrared Camera (Fazio et al. 2004) have provided some constraints on the vigor of atmospheric mixing (e.g., Leggett et al. 2007).

<sup>4</sup> The error is derived solely from the error in  $C_k$  and therefore does not include any errors in  $T_{\text{eff}}$  and  $\log g$ .

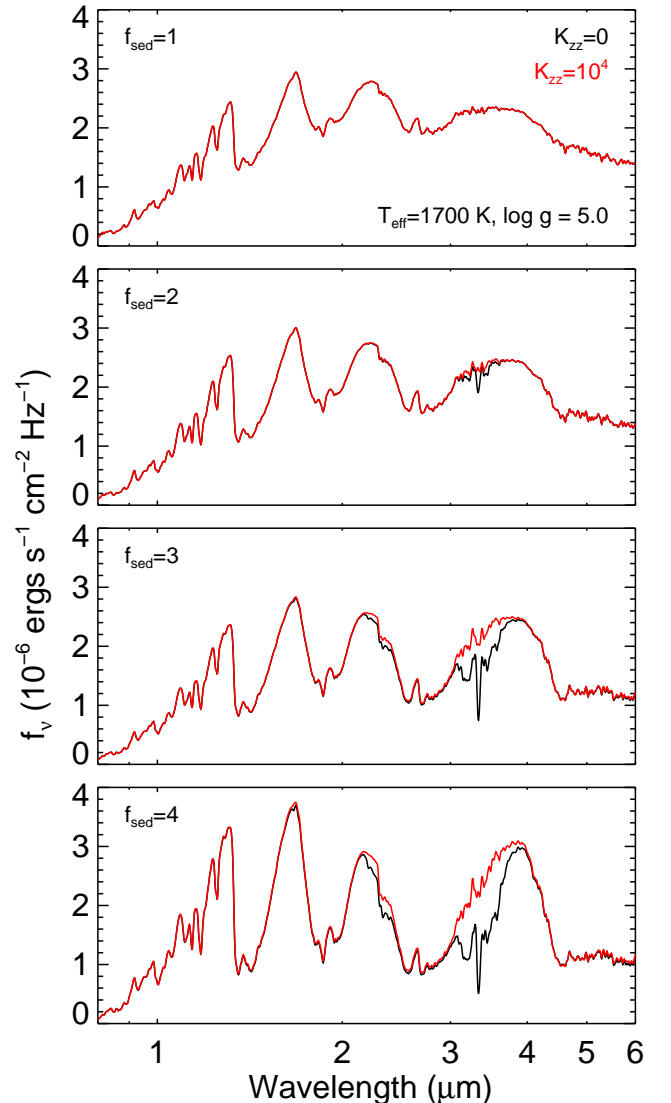


FIG. 3.— Comparison of the effect of non-equilibrium chemistry on the band strength of the fundamental  $\text{CH}_4$  band at 3.3  $\mu\text{m}$  as a function of the sedimentation efficiency parameter  $f_{\text{sed}}$ . Each panel shows two model spectra with  $T_{\text{eff}}=1700$  K,  $\log g=5.0$  [ $\text{cm s}^{-2}$ ],  $[M/H]=0$ , and  $K_{zz}=0$  (black),  $10^4$  (red)  $\text{cm}^2 \text{s}^{-1}$  at a fixed  $f_{\text{sed}}$ . The flux density units correspond to the emergent flux at the top of the atmosphere.

In contrast, *L* band spectroscopy is relatively easy to obtain from the ground making the 3.3  $\mu\text{m}$  region an attractive alternative to the 4.7  $\mu\text{m}$  CO band. Figure 3 shows a sequence of model spectra with  $T_{\text{eff}}=1700$  K,  $\log g=5.0$  [ $\text{cm s}^{-2}$ ],  $f_{\text{sed}}=1,2,3,4$  and  $K_{zz}=0, 10^4 \text{ cm}^2 \text{ s}^{-1}$ . The 2–4  $\mu\text{m}$  spectral region forms above the cloud layer so as the condensate clouds becomes thinner ( $f_{\text{sed}}$  increases), these layers become cooler, resulting in an increase both the abundance and band strengths of  $\text{CH}_4$ . However, when the effects of vertical mixing are included ( $K_{zz} > 0$ ), the depths of the  $\text{CH}_4$  bands are weakened dramatically and are nearly independent of the cloud properties. The strong dependence of the strength of the 3.3  $\mu\text{m}$   $\text{CH}_4$  band on  $K_{zz}$  in L dwarfs with thin condensate clouds and the relative ease of obtaining spectra at these wavelengths suggests that the class of blue L dwarfs are

the best objects with which to constrain the vigor of vertical mixing in the atmospheres of L dwarfs.

We thank Sarah Schmidt for providing the NIR SpeX spectrum of SDSS 1416+13 and Brendan Bowler and Mike Liu for useful discussions. This publication makes use of data from the Two Micron All Sky Survey, which is a joint project of the University of Massachusetts and the Infrared Processing and Analysis Center, and funded by the National Aeronautics and Space Administration and the National Science Foundation, the SIMBAD database, operated at CDS, Strasbourg, France, NASA's Astrophysics Data System Bibliographic Services, the M, L, and T dwarf compendium housed at DwarfArchives.org and maintained by Chris Gelino, Davy Kirkpatrick, and Adam Burgasser, and the NASA/ IPAC Infrared Science Archive, which is operated by the Jet Propulsion Laboratory, California Institute of Technology, under contract with the National Aeronautics and Space Administration. Support for the modeling work of D.S. was provided by NASA through the *Spitzer* Science Center.

*Facilities:* IRTF (SpeX)

## REFERENCES

- Ackerman, A. S., & Marley, M. S. 2001, *ApJ*, 556, 872
- Allard, F., Hauschildt, P. H., Alexander, D. R., Tamanai, A., & Schweitzer, A. 2001, *ApJ*, 556, 357
- Bowler, B. P., Liu, M. C., & Cushing, M. C. 2009, *ApJ*, 706, 1114
- Bowler, B. P., Liu, M. C., & Dupuy, T. J. 2010, *ApJ*, 710, 45
- Burgasser, A. J.,Looper, D., & Rayner, J. T. 2010, *AJ*, 139, 2448
- Burgasser, A. J.,Looper, D. L., Kirkpatrick, J. D., Cruz, K. L., & Swift, B. J. 2008a, *ApJ*, 674, 451
- Burgasser, A. J., Tinney, C. G., Cushing, M. C., Saumon, D., Marley, M. S., Bennett, C. S., & Kirkpatrick, J. D. 2008b, *ApJ*, 689, L53
- Burningham, B., et al. 2010a, *MNRAS*, 404, 1952
- , 2010b, *MNRAS*, 400
- Chiu, K., Fan, X., Leggett, S. K., Golimowski, D. A., Zheng, W., Geballe, T. R., Schneider, D. P., & Brinkmann, J. 2006, *AJ*, 131, 2722
- Cruz, K. L., et al. 2007, *AJ*, 133, 439
- Cruz, K. L., Reid, I. N., Liebert, J., Kirkpatrick, J. D., & Lowrance, P. J. 2003, *AJ*, 126, 2421
- Cushing, M. C., et al. 2008, *ApJ*, 678, 1372
- Cushing, M. C., Rayner, J. T., & Vacca, W. D. 2005, *ApJ*, 623, 1115
- Cushing, M. C., Vacca, W. D., & Rayner, J. T. 2004, *PASP*, 116, 362
- Faherty, J. K., Burgasser, A. J., Cruz, K. L., Shara, M. M., Walter, F. M., & Gelino, C. R. 2009, *AJ*, 137, 1
- Fazio, G. G., et al. 2004, *ApJS*, 154, 10
- Folkes, S. L., Pinfield, D. J., Kendall, T. R., & Jones, H. R. A. 2007, *MNRAS*, 378, 901
- Geballe, T. R., Saumon, D., Golimowski, D. A., Leggett, S. K., Marley, M. S., & Noll, K. S. 2009, *ApJ*, 695, 844
- Helling, C., Klein, R., Woitke, P., Nowak, U., & Sedlmayr, E. 2004, *A&A*, 423, 657
- Helling, C., Oevermann, M., Lüttke, M. J. H., Klein, R., & Sedlmayr, E. 2001, *A&A*, 376, 194
- Helling, C., & Woitke, P. 2006, *A&A*, 455, 325
- Hubeny, I., & Burrows, A. 2007, *ApJ*, 669, 1248
- Kirkpatrick, J. D. 2005, *ARA&A*, 43, 195
- Kirkpatrick, J. D. 2008, in *Astronomical Society of the Pacific Conference Series*, Vol. 384, 14th Cambridge Workshop on Cool Stars, Stellar Systems, and the Sun, ed. G. van Belle, 85
- Kirkpatrick, J. D., et al. 2010, *ApJS*, 190, 100
- , 1999, *ApJ*, 519, 802
- Knapp, G. R., et al. 2004, *AJ*, 127, 3553
- Leggett, S. K., et al. 2010, *ApJ*, 710, 1627
- , 2009, *ApJ*, 695, 1517
- , 2002, *ApJ*, 564, 452
- Leggett, S. K., Saumon, D., Marley, M. S., Geballe, T. R., Golimowski, D. A., Stephens, D., & Fan, X. 2007, *ApJ*, 655, 1079
- Lindal, G. F., et al. 1981, *J. Geophys. Res.*, 86, 8721
- Marley, M. S., Seager, S., Saumon, D., Lodders, K., Ackerman, A. S., Freedman, R. S., & Fan, X. 2002, *ApJ*, 568, 335
- Noll, K. S., Geballe, T. R., Leggett, S. K., & Marley, M. S. 2000, *ApJ*, 541, L75
- Noll, K. S., Geballe, T. R., & Marley, M. S. 1997, *ApJ*, 489, L87
- Oppenheimer, B. R., Kulkarni, S. R., Matthews, K., & van Kerkwijk, M. H. 1998, *ApJ*, 502, 932
- Rayner, J. T., Cushing, M. C., & Vacca, W. D. 2009, *ApJS*, 185, 289
- Rayner, J. T., Toomey, D. W., Onaka, P. M., Denault, A. J., Stahlberger, W. E., Vacca, W. D., Cushing, M. C., & Wang, S. 2003, *PASP*, 115, 362
- Saumon, D., & Marley, M. S. 2008, *ApJ*, 689, 1327
- Saumon, D., Marley, M. S., Cushing, M. C., Leggett, S. K., Roellig, T. L., Lodders, K., & Freedman, R. S. 2006, *ApJ*, 647, 552
- Saumon, D., et al. 2007, *ApJ*, 656, 1136
- Saumon, D., Marley, M. S., Lodders, K., & Freedman, R. S. 2003, in *IAU Symposium*, Vol. 211, *Brown Dwarfs*, ed. E. Martín, 345
- Schmidt, S. J., West, A. A., Burgasser, A. J., Bochanski, J. J., & Hawley, S. L. 2010a, *AJ*, 139, 1045
- Schmidt, S. J., West, A. A., Hawley, S. L., & Pineda, J. S. 2010b, *AJ*, 139, 1808
- Scholz, R. 2010, *A&A*, 510, L8
- Stephens, D. C., et al. 2009, *ApJ*, 702, 154
- Testi, L. 2009, *A&A*, 503, 639
- Vacca, W. D., Cushing, M. C., & Rayner, J. T. 2003, *PASP*, 115, 389
- Woitke, P., & Helling, C. 2003, *A&A*, 399, 297
- , 2004, *A&A*, 414, 335